

## Metal-Ion Selectivity Produced by C-Alkyl Substituents on the Bridges of Chelating Ligands: The Importance of Short H–H Nonbonded van der Waals Contacts in Controlling Metal-Ion Selectivity. A Thermodynamic, Molecular Mechanics, and Crystallographic Study

Robert D. Hancock,<sup>\*,†</sup> Alvaro S. de Sousa,<sup>\*,‡</sup> George B. Walton,<sup>†,||</sup> and Joseph H. Reibenspies<sup>§</sup>

Department of Chemistry and Biochemistry, University of North Carolina at Wilmington, Wilmington, North Carolina 28403, Department of Chemistry, University of the Witwatersrand, Johannesburg 2050, South Africa, and Department of Chemistry, Texas A&M University, College Station, Texas 77843

Received February 7, 2007

The effect on metal-ion selectivity of the use of cyclohexenyl bridges in ligands in place of ethylene bridges is examined (selectivity is defined as the difference in  $\log K_1$  for one metal ion relative to that of another with the same ligand). The syntheses of *N,N'*-bis(2-hydroxycyclohexyl)ethane-1,2-diamine (Cy<sub>2</sub>-en), *N,N'*-bis(2-hydroxycyclohexyl)propane-1,3-diamine (Cy<sub>2</sub>-tn), and 1,7-bis(2-hydroxycyclohexyl)-1,4,7-triazaheptane (Cy<sub>2</sub>-dien) are reported. The crystal structures of [Cu(Cy<sub>2</sub>-tn)(H<sub>2</sub>O)](ClO<sub>4</sub>)<sub>2</sub> (**1**) and [Cu(Cy<sub>2</sub>-dien)](ClO<sub>4</sub>)<sub>2</sub> (**2**) are reported. Characteristics of **1**: monoclinic, *Pn* space group,  $a = 11.627(2)$  Å,  $b = 7.8950(10)$  Å,  $c = 12.737(8)$  Å,  $\beta = 98.15(3)^\circ$ ,  $Z = 2$ ,  $R = 0.0524$ . Characteristics of **2**: orthorhombic, *Pbca* space group,  $a = 21.815(16)$  Å,  $b = 8.525(7)$  Å,  $c = 25.404(14)$  Å,  $Z = 8$ ,  $R = 0.0821$ . Structure **1** has the Cu(II) atom coordinated in the plane of the ligand to the two N donors and two O donors, with a long bond to an axially coordinated water molecule. **2** has three N donors, and one hydroxyl O donor from the ligand is coordinated in the plane around the Cu(II) atom, with the second hydroxyl O donor of the ligand occupying an axial site with a long Cu–O bond. The salient feature of both structures is the short H–H nonbonded distance between H atoms on the cyclohexenyl bridges and H atoms on the ethylene bridges of the ligand. These short contacts are important in explaining the metal-ion selectivities of these ligands. Formation constants, determined by glass-electrode potentiometry, for the Cy<sub>2</sub>-en (Cu(II), Ni(II), Zn(II), Cd(II), Pb(II)), Cy<sub>2</sub>-dien (Cu(II), Zn(II), Cd(II), Pb(II)), and Cy<sub>2</sub>-tn (Cu(II), Zn(II), Cd(II)) complexes are reported. These all show a strong shift in selectivity toward smaller metal ions compared with the analogous ligands, where ethylene bridges are present in place of the cyclohexenyl bridges of the ligands studied here. Molecular mechanics (MM) calculations are used to analyze these changes in selectivity. These calculations show that the short H–H contacts become shorter with increasing metal-ion size, which is suggested as the cause of the shift in the selectivity of ligands in favor of smaller metal ions when ethylene bridges are replaced with cyclohexenyl bridges. MM calculations are also used to rationalize, in terms of short H–H contacts, the fact that when the chelate ring contains two neutral O donors, more stable complexes result with *cis* placement of the donor atoms on the cyclohexenyl bridge, but with two N donors, *trans* placement of the donor atoms results in more stable complexes.

### Introduction

The search for factors that control metal-ion selectivity has led to several rules for ligand design.<sup>1–9</sup> These include

the effect of the addition of groups bearing neutral oxygen donors<sup>1–5</sup> to ligands, which moves selectivity in the direction of relatively smaller metal ions. (Selectivity is defined as

\* To whom correspondence should be addressed. E-mail: hancockr@uncw.edu (R.D.H.), alvaro@aurum.wits.ac.za (A.S.deS.).

† University of North Carolina.

‡ University of the Witwatersrand.

|| Present address: The South Carolina Governor's School for Science and Mathematics, Hartsville, SC 29550.

§ Texas A&M University.

(1) Hancock, R. D.; Martell, A. E. *Chem. Rev.* **1989**, *89*, 1875.

(2) Martell, A. E.; Hancock, R. D. *Metal Complexes in Aqueous Solutions*; Plenum Press: New York, 1996.

(3) Hancock, R. D. *Analyst (Cambridge, U.K.)* **1997**, *122*, 51R.

(4) (a) Hancock, R. D.; Maumela, H.; de Sousa, A. S. *Coord. Chem. Rev.* **1996**, *148*, 315. (b) Hancock, R. D.; Bhavan, R.; Wade, P. W.; Boeyens, J. C. A.; Dobson, S. M. *Inorg. Chem.* **1989**, *28*, 187.

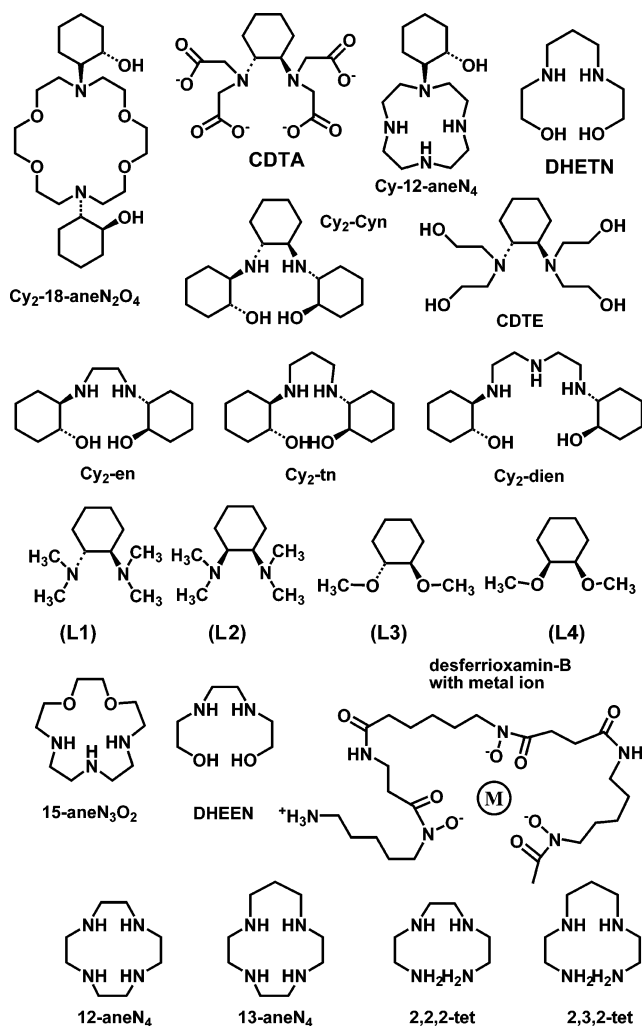


**Figure 1.** Ligands discussed in this paper. Note that where the ligand is indicated as a single enantiomer, it is actually the racemic mixture of both enantiomers.

the difference in  $\log K_1$  for the ligand with the metal ion of interest relative to that for competing metal ions, where  $\log K_1$  is the formation constant.) Another important factor is the affinity of metal ions for the  $\text{OH}^-$  ion,<sup>1–3,6,7</sup> which relates to the affinity that metal ions have for ligands such as ferrioxamin-B (see Figure 1 for key to ligand abbreviations), with its  $\text{RO}^-$  donor atoms. This can be expressed as a linear free-energy relationship (LFER) between  $\log K_1$  for ferrioxamin-B and  $\log K_1$  for  $\text{OH}^-$  for a wide variety of metal ions. A third factor is the size of the chelate ring.<sup>1–3,8–14</sup>

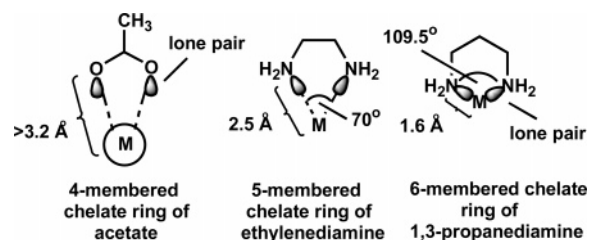


**Figure 2.** Examples of chelate rings with best-fit-size metal ions, showing diagrammatically how the bonding orbitals of the donor atoms in the chelate rings focus on smaller metal ions as the size of the chelate ring increases. The M–L bond lengths and L–M–L angles for best-fit metal ions are shown for each ring.

The increase in size of the chelate ring from the five-membered to the six-membered ring increases the selectivity for relatively smaller metal ions. This is a powerful ligand design tool and has been recently<sup>14</sup> used to design a fluorescent ligand that is selective for smaller metal ions such as Zn(II) over larger metal ions such as Cd(II) and Pb(II). In short, as shown in Figure 2, the lone pairs on the donor atoms of larger chelate rings, in the conformation required to form the chelate ring, focus on smaller metal ions. The definitions of metal-ion size used here are in terms of the ionic radius,  $r^+$ :<sup>15</sup> very large,  $r^+ \geq 1.2 \text{ \AA}$ ; large,  $1.2 > r^+ > 1.0 \text{ \AA}$ ; medium,  $1.0 > r^+ > 0.8 \text{ \AA}$ ; medium–small,  $0.8 > r^+ > 0.7 \text{ \AA}$ ; small,  $0.7 > r^+ > 0.5 \text{ \AA}$ ; very small,  $r^+ < 0.5 \text{ \AA}$ .

Chelate ring size is a dominant architectural feature in ligand design.<sup>1–3,8–14</sup> Molecular mechanics (MM) studies<sup>1–3,16,17</sup> have shown that tetraaza macrocycles, for example, can assume several energetically similar conformers that can accommodate metal ions of different sizes, so that the anticipated “hole-size” control of selectivity is not observed.<sup>1–3,16,17</sup> The metal-ion selectivity patterns of tetraaza macrocycles differ little from those of their open-chain polyamine analogues, and the controlling factor is chelate ring size. Thus, replacing the five-membered chelate rings in 12-aneN<sub>4</sub> to give 13-aneN<sub>4</sub> or in 2,2,2-tet to give 2,3,2-tet produces a nearly identical change in selectivity such that the increase in the size of the chelate ring from five-membered to six-membered causes a shift in selectivity in favor of smaller metal ions.<sup>1,8</sup>

The rules described above can be analyzed statistically through LFERs. Thus, Figure 3 shows a LFER of  $\Delta \log K$  for the *trans*-DM-EDTA and DM-TMDTA pair of ligands as a function of metal-ion radius ( $r^+$ ).<sup>15</sup> There is an increase in chelate ring size from five-membered size to six-membered size in passing from *trans*-DM-EDTA to DM-TMDTA. As the metal-ion radius increases, there is a decrease in  $\log K_1$  for DM-TMDTA relative to that of *trans*-DM-EDTA, in accordance with the chelate ring size rule. A least-squares best-fit line has been fitted to the relationship using EXCEL,<sup>18</sup> which facilitates statistical analysis and the

- (5) (a) Clapp, L. A.; Siddons, C. J.; Vanderveer, D. J.; Rogers, R. D.; Griffin, S. F.; Whitehead, J. R.; Jones, S. B.; Hancock, R. D. *Inorg. Chem.* **2005**, *44*, 8945. (b) Clapp, L. M.; Vanderveer, D. J.; Jones, S. B.; Hancock, R. D. *Dalton Trans.* **2006**, 2001.  
 (6) Evers, A.; Hancock, R. D.; Martell, A. E.; Motekaitis, R. J. *Inorg. Chem.* **1989**, *28*, 2189.  
 (7) Jarvis, N. V.; Hancock, R. D. *Inorg. Chim. Acta* **1991**, *182*, 229.  
 (8) Thom, V. J.; Hosken, G. D.; Hancock, R. D. *Inorg. Chem.* **1985**, *24*, 3378.  
 (9) Hancock, R. D. *Acc. Chem. Res.* **1990**, *26*, 253.  
 (10) Hancock, R. D.; Martell, A. E. *Comments Inorg. Chem.* **1988**, *6*, 237.  
 (11) Hancock, R. D.; Wade, P. W.; Ngwenya, M. P.; de Sousa, A. S.; Damu, K. V. *Inorg. Chem.* **1990**, *29*, 1968.  
 (12) Hancock, R. D. *J. Chem. Educ.* **1992**, *69*, 615.  
 (13) Cukrowski, I.; Cukrowska, E.; Hancock, R. D.; Anderegg, G. *Anal. Chim. Acta* **1995**, *312*, 307.

- (14) Gan, W.; Jones, S. B.; Reibenspies, J. H.; Hancock, R. D. *Inorg. Chim. Acta* **2005**, *358*, 3958.  
 (15) Shannon, R. D. *Acta Crystallogr.* **1976**, *A32*, 751.  
 (16) Thöm, V. J.; Fox, C. C.; Boeyens, J. C. A.; Hancock, R. D. *J. Am. Chem. Soc.* **1984**, *106*, 5947.  
 (17) Hancock, R. D. *Prog. Inorg. Chem.* **1989**, *37*, 187.  
 (18) Billo, E. J. *EXCEL for Chemists*; Wiley-VCH: New York, 2001.

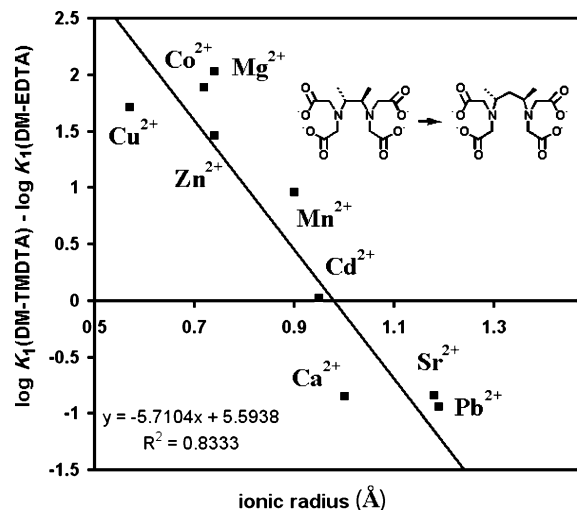


**Figure 3.** LFER showing metal-ion size-related change in selectivity ( $\Delta \log K$ ) for  $M^{2+}$  ions as a function of metal-ion radius<sup>15</sup> as chelate ring size is increased from *trans*-DM-EDTA (five-membered central chelate ring) to DM-TMDTA (six-membered central chelate ring) complexes.  $\Delta \log K$  refers to the equilibrium:  $M(\textit{trans}\text{-DM-EDTA}) + \text{DM-TMDTA} \rightleftharpoons M(\text{DM-TMDTA}) + \textit{trans}\text{-DM-EDTA}$ .  $\log K_1$  data from ref 19. Ionic radii<sup>15</sup> for octahedral metal ions except for Cu(II), for which the square-planar radius is given.

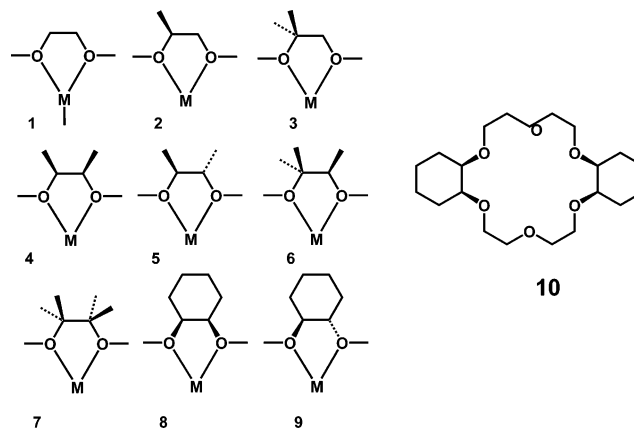
calculation of coefficients of determination ( $R^2$ ) for the relationships. For dozens of such relationships,  $R^2$  values of better than 0.8 are obtained.

An interesting effect on metal-ion selectivity is seen for ligands containing cyclohexylene bridges,<sup>20–22</sup> as in the examples of such ligands shown in Figure 1. It is perhaps surprising that, compared with the ethylene bridge, the rigid cyclohexylene bridge consistently leads<sup>3,20–22</sup> to a shift in selectivity in the direction of smaller metal ions, since the cyclohexylene bridge also involves a five-membered chelate ring. This resembles the effect of substituting H atoms on the bridges of the chelate rings of EDTA with C-alkyl groups,<sup>3</sup> which also leads to a shift in selectivity in the direction of smaller metal ions. This is illustrated in Figure 4 for isopropyl-EDTA, where the bulky isopropyl group on the central bridge of the ligand leads to a shift in selectivity in the direction of smaller metal ions as compared with the unsubstituted EDTA ligand.

Some metal-ion complexing properties of the ligands *N,N'*-bis(2-hydroxycyclohexyl)ethane-1,2-diamine ( $Cy_2\text{-en}$ ), *N,N'*-bis(2-hydroxycyclohexyl)propane-1,3-diamine ( $Cy_2\text{-tn}$ ), and 1,7-bis(2-hydroxycyclohexyl)-1,4,7-triazaheptane ( $Cy_2\text{-dien}$ ) are reported here, with the aim being to further analyze the effects of cyclohexylene bridges and other C-alkyl groups placed on the bridges of chelating ligands on metal-ion size-based selectivity.  $Cy_2\text{-dien}$  has the same donor set as the macrocycle 15-ane- $N_3O_2$  reported earlier,<sup>4,23,24</sup> and a com-

parison can be made of the selectivity effects induced by the cyclohexylene groups of  $Cy_2\text{-dien}$  as compared with the macrocyclic ring of 15-ane $N_3O_2$ .  $Cy_2\text{-tn}$  is of interest because it combines two features, the cyclohexylene groups and a six-membered chelate ring, in its complexes, which should lead to selectivity for smaller metal ions as compared with  $Cy_2\text{-en}$ . The structures of  $[\text{Cu}(\text{Cy}_2\text{-tn})(\text{H}_2\text{O})](\text{ClO}_4)_2$  (**1**) and  $[\text{Cu}(\text{Cy}_2\text{-dien})](\text{ClO}_4)_2$  (**2**) were determined to examine structural features of these complexes that might relate to the selectivity patterns exhibited, particularly the presence of H–H nonbonded interactions in the coordinated ligands.

The effects of C-alkyl substituents, including cyclohexenyl groups, on the ethylene bridges of crown ethers complexing with alkali-metal ions have been studied by Hay et al.<sup>25</sup> In this elegant study, MM calculations on complexes of alkali-metal ions with the  $\text{CH}_3\text{OCH}_2\text{CH}_2\text{OCH}_3$  type of ligand with various alkyl substituents on the ethylene bridges were used to predict the metal-ion affinities of crown ethers bearing the same substituents on some of their ethylene bridges. The substituted ethylene bridges studied<sup>25</sup> are summarized in the diethers 1–9 in the following graphic.



The idea here was that an analysis of the complexes of the above diethers 1–9 would predict metal-ion selectivity patterns of sets of crown ethers containing one or two such bridges. Thus, the selectivity patterns of crown ether 10 relative to those of other crown ethers with two bridges, corresponding to those in the diethers 1–9, could be predicted by considering the selectivity effects of 8 on its own compared with the other diethers. It was found that this approach successfully predicted the metal-ion affinities of crown ethers. However, in contrast to what has been found previously<sup>20–22</sup> with N-donor ligands, the study of Hay et al. predicted, as supported by experimental  $\log K_1$  values,<sup>26</sup> that for alkali-metal ions with crown ethers, alkyl substituents on the ethylene bridges led to drops in  $\log K_1$  values. The explanation for this advanced by Hay et al. was that alkyl substituents caused less favorable conformations of the chelate rings to be adopted and thereby destabilized the

(19) Martell, A. E.; Smith, R. M. *Critical Stability Constant Database*; National Institute of Science and Technology: Gaithersburg, MD, 2003; Vol. 46.

(20) De Sousa, A. S.; Croft, G. J. B.; Wagner, C. A.; Michael, J. P.; Hancock, R. D. *Inorg. Chem.* **1991**, *30*, 3525.

(21) De Sousa, A. S.; Hancock, R. D.; Reibenspies, J. H. *J. Chem. Soc., Dalton Trans.* **1997**, 939.

(22) De Sousa, A. S.; Hancock, R. D.; Reibenspies, J. H. *J. Chem. Soc., Dalton Trans.* **1997**, 2831.

(23) Cabral, M. F.; Delgado, R. *Helv. Chim. Acta* **1994**, *77*, 515.

(24) Bazziculi, C.; Bencini, A.; Bianchi, A.; Fusi, V.; Giorgi, C.; Paoletti, P.; Valtancoli, B.; Zanchi, D. *Inorg. Chem.* **1997**, *36*, 2784.

(25) Hay, B. P.; Zhang, D.; Rustad, J. R. *Inorg. Chem.* **1996**, *35*, 2650.

(26) Izatt, R. M.; Pawlak, K.; Bradshaw, K. S.; Bruening, R. L. *Chem. Rev.* **1991**, *91*, 1721; **1995**, *95*, 2529.

**Table 1.** Crystallographic Data for **1** and **2**

|                             | <b>1</b>   | <b>2</b>   |
|-----------------------------|--|--|
| empirical formula           | C <sub>15</sub> H <sub>32</sub> Cl <sub>2</sub> CuN <sub>2</sub> O <sub>11</sub> | C <sub>16</sub> H <sub>33</sub> Cl <sub>2</sub> CuN <sub>3</sub> O <sub>10</sub> |
| <i>M</i>                    | 552.87   | 561.89   |
| <i>T</i> (K)                | 163(2)   | 293(2)   |
| cryst syst                  | monoclinic   | orthorhombic   |
| space group                 | <i>Pn</i>  | <i>Pbca</i>  |
| <i>a</i> (Å)                | 11.627(2)  | 21.815(16)   |
| <i>b</i> (Å)                | 7.895(1)   | 8.525(7)   |
| <i>c</i> (Å)                | 12.737(8)  | 25.404(14)   |
| $\alpha$ (deg)              | 90   | 90   |
| $\beta$ (deg)               | 98.15(3)   | 90   |
| $\gamma$ (deg)              | 90   | 90   |
| <i>U</i> (Å <sup>3</sup> )  | 1157.4(8)  | 4724.5(58)   |
| <i>Z</i>                    | 2  | 8  |
| $\mu$ (mm <sup>-1</sup> )   | 1.231  | 1.206  |
| reflins collected           | 2161   | 4104   |
| independent reflns          | 2003   | 4072   |
| final <i>R</i> indices      | R1 = 0.0524,   | R1 = 0.0821,   |
| $[I \geq 2\sigma(I)]$       | wR2 = 0.1359   | wR2 = 0.2058   |
| <i>R</i> indices (all data) | R1 = 0.0619,   | R1 = 0.2302,   |
|                             | wR2 = 0.1594   | wR2 = 0.3743   |

complexes. Of particular interest is the fact that groups such as the *trans*-cyclohexylene bridge (diether **9** in the graphic above) produce the largest decrease in log *K*<sub>1</sub> with crown ethers,<sup>25,26</sup> whereas with ligands such as those reported here with N donors, the *trans*-cyclohexylene bridge produces the greatest increase in log *K*<sub>1</sub>. In addition, a *cis* arrangement of the O-donor atoms on cyclohexylene bridges in crown ethers (structure **8** in the graphic) leads to more stable complexes than a *trans* arrangement, whereas for the N-donor ligands studied here, the opposite is true. In this paper we attempt to explain why cyclohexylene bridges could produce such differing effects in different ligand systems. The specific questions that are raised here are as follows: (1) Why are complexes where the substituents on the bridge are *trans* and where there are N donors in the chelate ring more stable than *cis*-substituted analogues, compared with ligands that contain only neutral O donors, where the reverse is true. For the latter types of ligand, studied by Hay et al., that have only neutral O-donors, *trans*-substituted cyclohexylene bridges produce complexes of lower stability than any other pattern of substitution, whereas the *cis*-substituted analogues are of the highest stability. (2) What causes the selectivity of ligands to shift in favor of smaller metal ions when alkyl substituents are added to bridges between two N donors or an N donor and a neutral O donor? The work of Hay et al.<sup>25</sup> suggests that the preference of ligands containing neutral O donors will always be for larger metal ions, regardless of the substitution pattern on the bridge of the ligand. (3) Why does the addition of C-alkyl groups to ethylene bridges between an N-donor or between an N donor and an O donor cause an increase in log *K*<sub>1</sub> compared with that of the unsubstituted ligand, and why do all such substitutions on chelate rings involving only neutral oxygen donors usually lead to a drop, or at best a marginal increase, in complex stability?

## Experimental Section

**Materials.** Metal nitrates and perchlorates were obtained from Aldrich in at least 99% purity and were used as received.

**Synthesis of *N,N'*-bis(2-hydroxycyclohexyl)ethylenediamine (C<sub>2</sub>-en).** Ethylenediamine (SAARCHEM, 1.0 g) was dissolved in

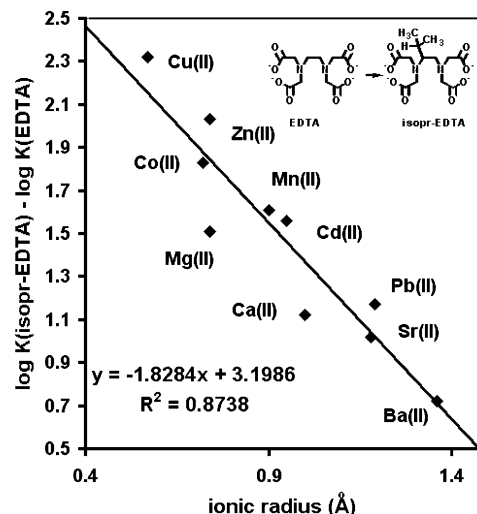


**Figure 4.** LFER showing for  $M^{2+}$  ions the metal-ion size-related change in selectivity ( $\Delta \log K$ , which here is  $\log K(\text{isopropyl-EDTA}) - \log K(\text{EDTA})$ ) as a function of metal-ion radius for isopropyl-EDTA relative to that of EDTA. Ionic radii<sup>15</sup> for octahedral metal ions except for Cu(II), for which the square-planar radius is given. Least-squares best-fit line and its equation, plus  $R^2$ , calculated using EXCEL.<sup>18</sup>

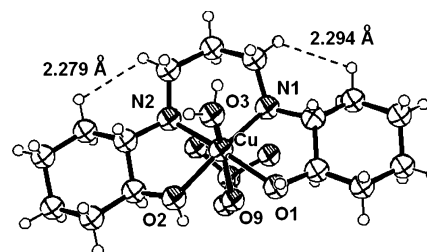


**Figure 5.** ORTEP drawing of the complex cation of **1**, showing the numbering scheme for atoms coordinated to the Cu atom. The atom O(9) is from a coordinated perchlorate, whereas O(3) is from a coordinated water molecule. Short H–H nonbonded separations discussed in the text are indicated as broken lines.

60 mL of anhydrous ethanol, and to this was added cyclohexene oxide (Fluka, 6.5 g). The solution was refluxed for 6 h in a round-bottomed flask fitted with a CaCl<sub>2</sub> drying tube. A white precipitate formed, which was collected and air-dried. After further refluxing, the solvent was removed, and an oil was obtained that solidified on standing. The solids were combined and crystallized from 50 mL of acetone to give 3.4 g of crystalline material (yield = 80%). <sup>1</sup>H NMR (D<sub>2</sub>O):  $\delta_{\text{H}}$  3.32 (m, 2H, CHOH), 2.61 (m, 4H, CH<sub>2</sub>NHR), 2.36 (m, 2H, CHNHR), 1.94 (br s, 4H, CH<sub>2</sub>CHOH), 1.67 (br s, 4H, CH<sub>2</sub>CHNHR), 1.22 (br m, 8H, CH<sub>2</sub>CH<sub>2</sub>CH<sub>2</sub>CH<sub>2</sub>). <sup>13</sup>C NMR (CDCl<sub>3</sub>):  $\delta_{\text{C}}$  74.90 (CHOH), 64.06 (CHNHR), 47.47 (CH<sub>2</sub>NHR), 33.81 (CH<sub>2</sub>CHOH), 31.62 (CH<sub>2</sub>CHNHR), 25.61 (CH<sub>2</sub>CH<sub>2</sub>CH<sub>2</sub>CH<sub>2</sub>). MS (FAB, NBA): *m/z* 257.2 ( $M^+ + 1$ ). Anal. Calcd for C<sub>14</sub>H<sub>28</sub>N<sub>2</sub>O<sub>2</sub>: C, 65.59; H, 11.01; N, 10.93. Found: C, 65.58; H, 11.23; N, 10.93.

**Synthesis of *N,N'*-Bis(2-hydroxycyclohexyl)-1,3-propanediamine (C<sub>2</sub>-tn).** 1,3-Propanediamine (Aldrich, 1.0 g) was dissolved in 60 mL of anhydrous ethanol, and to this was added cyclohexene oxide (Fluka, 5.3 g). The solution was refluxed at 80 °C for 24 h in a round-bottomed flask fitted with a CaCl<sub>2</sub> drying tube. After refluxing, the solvent was removed and an oil was obtained that solidified on drying under reduced pressure. The solid was crystallized from 35 mL acetone to give 2.9 g of crystalline material (yield = 80%). <sup>1</sup>H NMR (D<sub>2</sub>O):  $\delta_{\text{H}}$  3.30 (m, 2H, CHOH), 2.69 (m, 2H, CH<sub>2</sub>NHR), 2.56 (m, 2H, CH<sub>2</sub>NHR), 2.35 (m, 2H, CHNHR), 1.92 (br d, 4H, CH<sub>2</sub>CHOH), 1.67 (br m, 6H, CH<sub>2</sub>CHNHR and CH<sub>2</sub>-



**Table 2.** Selected Bond Lengths and Angles for **1**

|                 |          | Bond Lengths (Å)  |          |            |          |
|-----------------|----------|-------------------|----------|------------|----------|
| Cu(1)–N(1)      | 1.977(9) | Cu(1)–O(2)        | 1.992(9) | Cu(1)–O(1) | 1.996(6) |
| Cu(1)–N(2)      | 1.998(7) | Cu(1)–O(3)        | 2.263(9) | Cu(1)–O(9) | 2.789(9) |
|                 |          | Bond Angles (deg) |          |            |          |
| N(1)–Cu(1)–O(2) | 172.8(4) | N(1)–Cu(1)–O(1)   |          |            | 84.5(3)  |
| O(2)–Cu(1)–O(1) | 94.9(3)  | N(1)–Cu(1)–N(2)   |          |            | 94.5(3)  |
| O(2)–Cu(1)–N(2) | 85.0(3)  | O(1)–Cu(1)–N(2)   |          |            | 170.9(3) |
| N(1)–Cu(1)–O(3) | 97.2(4)  | O(2)–Cu(1)–O(3)   |          |            | 90.0(4)  |
| O(1)–Cu(1)–O(3) | 91.8(3)  | N(2)–Cu(1)–O(3)   |          |            | 97.3(3)  |

CH<sub>2</sub>NHR), 1.39–0.92 (br m, 8H, CH<sub>2</sub>CH<sub>2</sub>CH<sub>2</sub>CH<sub>2</sub>). <sup>13</sup>C NMR (CDCl<sub>3</sub>): δ<sub>C</sub> 73.55 (CHOH), 63.58 (CHNHR), 45.25 and 44.95 (CH<sub>2</sub>NHR), 33.54 (CH<sub>2</sub>CHOH), 30.47 (CH<sub>2</sub>CHNHR), 25.06 (CH<sub>2</sub>–CH<sub>2</sub>NHR), 24.42 (CH<sub>2</sub>CH<sub>2</sub>CH<sub>2</sub>CH<sub>2</sub>). MS (FAB, NBA): *m/z* 271.2 (M<sup>+</sup> + 1). Anal. Calcd for C<sub>15</sub>H<sub>30</sub>N<sub>2</sub>O<sub>2</sub>: C, 66.63; H, 11.18; N, 10.35. Found: C, 65.58; H, 11.71; N, 10.31.

**Synthesis of *N,N'*-Bis(2-hydroxycyclohexyl)diethylenetriamine (Cy<sub>2</sub>-dien).** Diethylenetriamine (Riedel de Haan, 2.0 g) was dissolved in 60 mL of anhydrous ethanol, and to this was added cyclohexene oxide (Fluka, 9.5 g). The solution was refluxed for 24 h in a round-bottomed flask fitted with a CaCl<sub>2</sub> drying tube, after which the solvent was removed and a pale-yellow oil was obtained that solidified on drying under reduced pressure. The solid was crystallized from 50 mL of hot acetone to give 3.3 g of crystalline material (yield = 57%). <sup>1</sup>H NMR (D<sub>2</sub>O): δ<sub>H</sub> 3.28 (m, 2H, CHOH), 2.68 (m, 8H, CH<sub>2</sub>NHR), 2.34 (m, 2H, CHNHR), 1.94 (br d, 4H, CH<sub>2</sub>CHOH), 1.66 (br s, 4H, CH<sub>2</sub>CHNHR), 1.38–0.89 (br m, 8H, CH<sub>2</sub>CH<sub>2</sub>CH<sub>2</sub>CH<sub>2</sub>). <sup>13</sup>C NMR (CDCl<sub>3</sub>): δ<sub>C</sub> 73.59 (CHOH), 63.52 (CHNHR), 49.81 and 45.89 (CH<sub>2</sub>NHR), 33.73 (CH<sub>2</sub>CHOH), 30.79 (CH<sub>2</sub>CHNHR), 24.99 and 24.52 (CH<sub>2</sub>CH<sub>2</sub>CH<sub>2</sub>–CH<sub>2</sub>). MS (FAB, NBA): *m/z* 300.1 (M<sup>+</sup> + 1). Anal. Calcd for C<sub>16</sub>H<sub>33</sub>N<sub>3</sub>O<sub>2</sub>: C, 64.16; H, 11.11; N, 14.03. Found: C 64.61; H, 11.54; N, 13.81.

**Synthesis of [Cu(Cy<sub>2</sub>-tn)(H<sub>2</sub>O)](ClO<sub>4</sub>)<sub>2</sub> (**1**).** The ligand (0.4 g) in 10 mL deionized water was added to Cu(ClO<sub>4</sub>)<sub>2</sub>·6H<sub>2</sub>O (Aldrich, 0.5 g) in 20 mL of deionized water after the addition of 10 mL of a solution of KOH (0.15 g) and cooling in an ice bath. After warming (60–65 °C) for 20 min, the complex precipitated as dark-blue crystals (wt. of product = 0.82 g; yield = 58%). Anal. Calcd for C<sub>15</sub>H<sub>30</sub>N<sub>2</sub>O<sub>11</sub>Cl<sub>2</sub>Cu: C, 32.59; H, 5.83; N, 5.07. Found: C, 33.38; H, 5.71; N, 5.46.

**Synthesis of [Cu(Cy<sub>2</sub>-dien)](ClO<sub>4</sub>)<sub>2</sub> (**2**).** The ligand (0.6 g) in 10 mL of deionized water was added to Cu(ClO<sub>4</sub>)<sub>2</sub>·6H<sub>2</sub>O (Aldrich, 0.7 g) in 15 mL of deionized water after the addition of 10 mL of a solution of KOH (0.2 g) and cooling in an ice bath. After warming (70 °C) for 20 min, the complex precipitated on cooling as dark-blue crystals (wt. of product = 0.73 g; yield = 65%). Anal. calcd for C<sub>16</sub>H<sub>33</sub>N<sub>3</sub>O<sub>10</sub>Cl<sub>2</sub>Cu: C, 34.20; H, 5.92; N, 7.48. Found: C, 33.95; H, 5.75; N, 7.16.

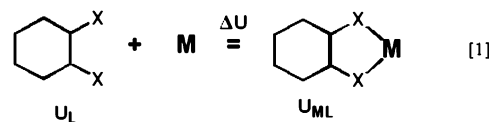
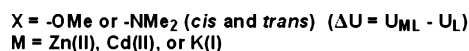
**Molecular Structure Determination.** A mounted crystal of **1** was placed in a cold nitrogen stream maintained at –80 °C. A Rigaku AFC5 four-circle diffractometer was employed for crystal screening, unit cell determination, and data collection for both structures. The structure was solved by Patterson synthesis and refined to convergence.<sup>27</sup> Details of the structure determinations of **1** and **2** are shown in Table 1, and these together with the crystal coordinates have been deposited with the CCDC.<sup>28</sup> Some more important bond lengths and angles for **1** and **2** are given in Tables 2 and 3.

(27) G. M. Sheldrick. *SHELX 5.1*; Bruker AXS, Inc.: Madison, WI, 1998.

(28) Cambridge Crystallographic Data Centre, 12 Union Road, Cambridge CB2 1EZ, United Kingdom.

**Formation Constant Determination.** Formation constants were determined by glass-electrode potentiometry following literature methods.<sup>29</sup> Potentiometric measurements were made with a Radiometer PHM84 pH meter equipped with a combined glass/reference electrode (GK2402B or GK2401C). Potentiometric data were analyzed using the *ESTA* program.<sup>30</sup> The potentiometric studies were carried out in 0.1 M NaNO<sub>3</sub>, and all solutions were thermostatted to 25.0 ± 0.1 °C during potentiometric studies. Formation constants reported here for the complexes of Cy<sub>2</sub>-en, Cy<sub>2</sub>-tn, and Cy<sub>2</sub>-dien are given in Table 4.

**MM Calculations.** These were carried out using the program *HyperChem*,<sup>31</sup> which utilizes the MM+ force field, which is an expanded version of the MM2 force field,<sup>32</sup> and was used for all MM calculations using the default parameters in the program. MM was used to calculate the increase in strain energy (Δ*U*) of the ligand on complex formation,<sup>16</sup> using –OMe (Me = methyl) or –NMe<sub>2</sub> groups on model chelate rings much in the manner of Hay et al.<sup>25</sup> The ligands used as models were thus L1, L2, L3, and L4 in Figure 1. The strain energies of the free ligands and of the complexes with K(I), Cd(II), and Zn(II) were calculated to obtain Δ*U* from eq 1:



Hay et al. carried out an extensive search for the minimum strain energy conformers of the metal-ion complexes and the free ligands, and it was found for cyclohexylene bridges, both cis and trans substituted, that what was termed the (0 + 0) conformer for the positions of the MeO– groups was of the lowest strain energy in all cases. The full meaning of this terminology is given in their paper,<sup>25</sup> but describing it simply here, the conformers have the O–C bonds of the methoxy groups approximately parallel to the C–C bond of the bridge between the two O-donor atoms, as seen in parts c and d of Figure 9 in the Results and Discussion section. In fact, if one assumes that the cyclohexenyl bridge will adopt a chair conformation, very few conformations are actually possible even for the free ligand. These involve different orientations of the MeO– groups, and MM calculations here, experimenting with different orientations of the MeO– groups, support the idea that the (0 + 0) conformation is of the lowest energy for cyclohexenyl bridges. For cyclohexenyl-bridged ligands with –NMe<sub>2</sub> groups (L1 and L2 in Figure 1), only one low-energy conformer for the complexes and

(29) Martell, A. E.; Motekaitis, R. J. *Determination and Use of Stability Constants*; VCH Publishers: New York, 1989.

(30) May, P. M.; Murray, K.; Williams, D. R. *Talanta* **1985**, *32*, 483.

(31) *HyperChem* program, version 7.5; Hypercube, Inc.: Waterloo, ONT, Canada.

(32) Allinger, N. L. *J. Am. Chem. Soc.* **1977**, *98*, 8127.

**Table 3.** Selected Bond Lengths and Angles for **2**

| Bond Lengths (Å)  |          |                 |          |
|-------------------|----------|-----------------|----------|
| Cu(1)–N(2)        | 1.963(9) | Cu(1)–O(1)      | 1.991(6) |
| Cu(1)–N(1)        | 1.997(7) | Cu(1)–N(3)      | 2.033(8) |
| Cu(1)–O(2)        | 2.241(7) |                 |          |
| Bond Angles (deg) |          |                 |          |
| N(2)–Cu(1)–O(1)   | 148.1(3) | N(2)–Cu(1)–N(1) | 86.1(4)  |
| O(1)–Cu(1)–N(1)   | 83.7(3)  | N(2)–Cu(1)–N(3) | 87.3(4)  |
| O(1)–Cu(1)–N(3)   | 104.7(3) | N(1)–Cu(1)–N(3) | 171.5(3) |
| N(2)–Cu(1)–O(2)   | 118.2(3) | O(1)–Cu(1)–O(2) | 93.2(3)  |
| N(1)–Cu(1)–O(2)   | 98.3(3)  | N(3)–Cu(1)–O(2) | 80.1(3)  |

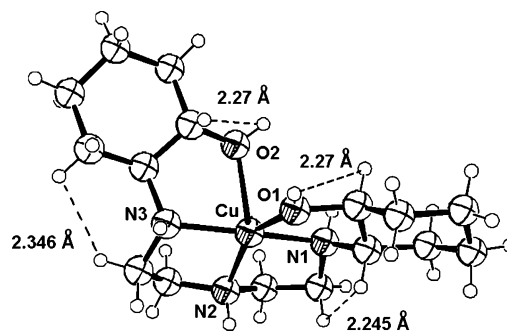
free ligands occurs, and it is that seen in parts a and b of Figure 9.

To scan strain energy as a function of metal-ion size,<sup>33</sup> the force constants involving the metal ion were kept constant at those for high-spin Ni(II), and the strain-free M–N and M–O bond lengths were varied over a range from 1.9 to 3.2 Å. The ideal M–O length at each point was set to be 0.06 Å shorter than the ideal M–N length, which is a typical difference in bond length for any one metal ion.

## Results and Discussion

**Structures of Complexes.** The structures of the complex cations  $[\text{Cu}(\text{Cy}_2\text{-tn})(\text{H}_2\text{O})]^{2+}$  and  $[\text{Cu}(\text{Cy}_2\text{-dien})]^{2+}$  from **1** and **2** are seen in Figures 5 and 6. The coordination around the Cu(II) atom in **1** consists of donor atoms from the  $\text{Cy}_2\text{-tn}$  ligand lying in the plane, with oxygen donors from a coordinated water molecule and a perchlorate occupying the axial sites, with long Cu–O bonds. What is of interest are the short H–H nonbonded contacts between the H atoms on the cyclohexenyl bridges and the H atoms on the trimethylene bridge of the ligand. These H atoms approach each other to well within the sum of the van der Waals radii<sup>34</sup> of two nonbonded H atoms, namely, 2.40 Å. In **2** (Figure 6), one of the O donors from a cyclohexyl group occupies an axial coordination site with a long Cu–O bond of 2.241 Å. One notes that there are also short contacts between H atoms on the cyclohexenyl bridges of **2** and adjacent ethylene bridges of the ligand. That involving the cyclohexenyl bridge where the O donor occupies the axial coordination site is somewhat longer, but it should be noted that there is a second fairly short H–H contact at that site, which becomes shorter as the size of the metal ion is increased in MM calculations, as discussed below. Also of importance are the short H–H contacts on **2** between the H atoms of the coordinated hydroxyl groups and the H atoms on the cyclohexylene bridges, also indicated in Figure 6.

**Formation Constants.** The formation constants determined here for  $\text{Cy}_2\text{-en}$ ,  $\text{Cy}_2\text{-tn}$ , and  $\text{Cy}_2\text{-dien}$  are seen in Table 4. As has been found with the few examples available<sup>19–22</sup> of chelating ligands with *trans*-cyclohexylene bridges between the donor atoms, where at least one of the donors is an N donor, considerable stabilization is found relative to analogues with ethylene bridges, which is size related. This is illustrated for  $\text{Cy}_2\text{-en}$  relative to DHEEN, its analogue with only ethylene bridges, in Figure 7. Figure 7 shows that the two cyclohexylene bridges of  $\text{Cy}_2\text{-en}$  cause a strong shift in

**Figure 6.** ORTEP drawing of the complex cation of **2** showing the numbering scheme of atoms coordinated to the Cu atom. Short H–H nonbonded separations discussed in the text are indicated as broken lines.**Table 4.** Formation and Protonation Constants of Ligands Reported in This Study<sup>a</sup>

| equilibrium   | log <i>K</i> | ref       |
|---|--------------|-----------|
| $\text{H}^+ + \text{OH}^- \rightleftharpoons \text{H}_2\text{O}$          | 13.78        | 19        |
| L = $\text{Cy}_2\text{-en}$   |              |           |
| $\text{L} + \text{H}^+ \rightleftharpoons \text{LH}^+$                    | 9.66         | this work |
| $\text{LH}^+ + \text{H}^+ \rightleftharpoons \text{LH}_2^{2+}$            | 6.62         | this work |
| $\text{Cu}^{2+} + \text{L} \rightleftharpoons \text{CuL}^{2+}$            | 11.47        | this work |
| $\text{CuL}^{2+} + \text{OH}^- \rightleftharpoons \text{CuLOH}^+$         | 6.64         | this work |
| $\text{CuLOH}^+ + \text{OH}^- \rightleftharpoons \text{CuL}(\text{OH})_2$ | 4.59         | this work |
| $\text{Ni}^{2+} + \text{L} \rightleftharpoons \text{NiL}^{2+}$            | 7.77         | this work |
| $\text{Zn}^{2+} + \text{L} \rightleftharpoons \text{ZnL}^{2+}$            | 6.18         | this work |
| $\text{ZnL}^{2+} + \text{OH}^- \rightleftharpoons \text{ZnLOH}^+$         | 5.29         | this work |
| $\text{ZnLOH}^+ + \text{OH}^- \rightleftharpoons \text{ZnL}(\text{OH})_2$ | 4.17         | this work |
| $\text{Cd}^{2+} + \text{L} \rightleftharpoons \text{CdL}^{2+}$            | 5.69         | this work |
| $\text{CdL}^{2+} + \text{OH}^- \rightleftharpoons \text{CdLOH}^+$         | 4.02         | this work |
| $\text{Pb}^{2+} + \text{L} \rightleftharpoons \text{PbL}^{2+}$            | 6.56         | this work |
| $\text{PbL}^{2+} + \text{OH}^- \rightleftharpoons \text{PbLOH}^+$         | 5.37         | this work |
| L = $\text{Cy}_2\text{-tn}$   |              |           |
| $\text{L} + \text{H}^+ \rightleftharpoons \text{LH}^+$                    | 10.12        | this work |
| $\text{LH}^+ + \text{H}^+ \rightleftharpoons \text{LH}_2^{2+}$            | 8.21         | this work |
| $\text{Cu}^{2+} + \text{L} \rightleftharpoons \text{CuL}^{2+}$            | 12.67        | this work |
| $\text{Zn}^{2+} + \text{L} \rightleftharpoons \text{ZnL}^{2+}$            | 5.04         | this work |
| $\text{Cd}^{2+} + \text{L} \rightleftharpoons \text{CdL}^{2+}$            | 4.15         | this work |
| L = $\text{Cy}_2\text{-dien}$   |              |           |
| $\text{L} + \text{H}^+ \rightleftharpoons \text{LH}^+$                    | 9.85         | this work |
| $\text{LH}^+ + \text{H}^+ \rightleftharpoons \text{LH}_2^{2+}$            | 8.76         | this work |
| $\text{LH}_2^{2+} + \text{H}^+ \rightleftharpoons \text{LH}_3^{3+}$       | 3.84         | this work |
| $\text{Cu}^{2+} + \text{L} \rightleftharpoons \text{CuL}^{2+}$            | 16.74        | this work |
| $\text{Zn}^{2+} + \text{L} \rightleftharpoons \text{ZnL}^{2+}$            | 9.57         | this work |
| $\text{Cd}^{2+} + \text{L} \rightleftharpoons \text{CdL}^{2+}$            | 9.34         | this work |
| $\text{Pb}^{2+} + \text{L} \rightleftharpoons \text{PbL}^{2+}$            | 9.01         | this work |

<sup>a</sup> At 25 °C in 0.1 M  $\text{NaNO}_3$ .

selectivity for the small Cu(II) ion relative to that of the large Pb(II) ion. Figure 8 shows the metal-ion size-related change in selectivity for  $\text{Cy}_2\text{-dien}$  complexes as compared with those of the macrocycle 15-ane $\text{N}_3\text{O}_2$ . Figure 8 shows that the nonmacrocyclic ligand  $\text{Cy}_2\text{-dien}$  is more selective for smaller metal ions than the macrocycle 15-ane $\text{N}_3\text{O}_2$ , which relates to the strong selectivity for small metal ions produced in ligands by the presence of cyclohexylene bridges as well as the larger cavity size of the macrocycle. It appears from structural studies of complexes of metal ions with 15-ane- $\text{X}_5$ -type macrocycles ( $\text{X} = \text{O}, \text{N}$ ) that<sup>36–38</sup> Mn(II) may fit the cavity best. Mn(II) has an ionic radius<sup>15</sup> of 0.8 Å, and it

(33) Hancock, R. D. *Prog. Inorg. Chem.* **1989**, *37*, 187.

(34) Bondi, A. J. *Phys. Chem.* **1964**, *68*, 441.

(35) Farrugia, L. J. *ORTEP-3 for Windows*, version 1.08; *J. Appl. Crystallogr.* **1997**, *30*, 565.

(36) Riley, D. P.; Lennon, P. J.; Neumann, W. L.; Weiss, R. H. *J. Am. Chem. Soc.* **1997**, *119*, 6522.

(37) Deng, Y.; Burns, J. H.; Moyer, B. A. *Inorg. Chem.* **1995**, *34*, 209.

(38) Reid, H. O. N.; Kahwa, I. A.; White, A. J. P.; Williams, D. J. *Chem. Commun.* **1999**, 1565.

**Table 5.** Formation Constants for Cy<sub>2</sub>-en (Five-Membered Chelate Ring) and Cy<sub>2</sub>-tn (Six-Membered Chelate Ring) Showing Variation with Metal-Ion Radius<sup>15</sup>

|  | metal ion |        |        |
|--|-----------|--------|--------|
|  | Cu(II)    | Zn(II) | Cd(II) |
| ionic radius <sup>15</sup> (Å)         | 0.57      | 0.74   | 0.95   |
| log K <sub>1</sub> Cy <sub>2</sub> -en | 11.47     | 6.18   | 5.69   |
| log K <sub>1</sub> Cy <sub>2</sub> -tn | 12.67     | 5.04   | 4.15   |

**Table 6.** Strain Energies (*U*) Calculated by MM for Free Ligands and Chelate Rings of the Ligands Shown with Metal Ions = Zn(II), Cd(II), and K(I)<sup>a</sup>

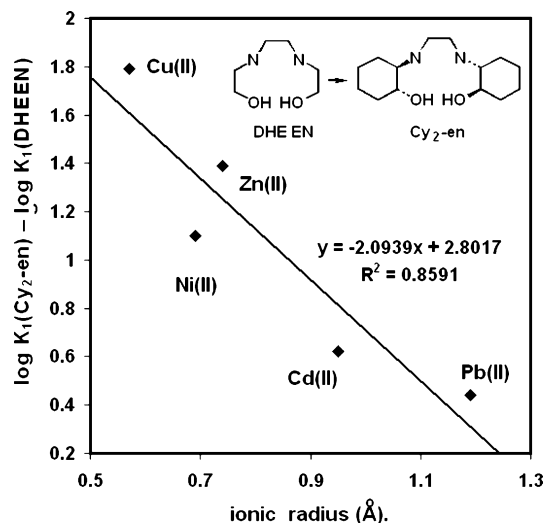
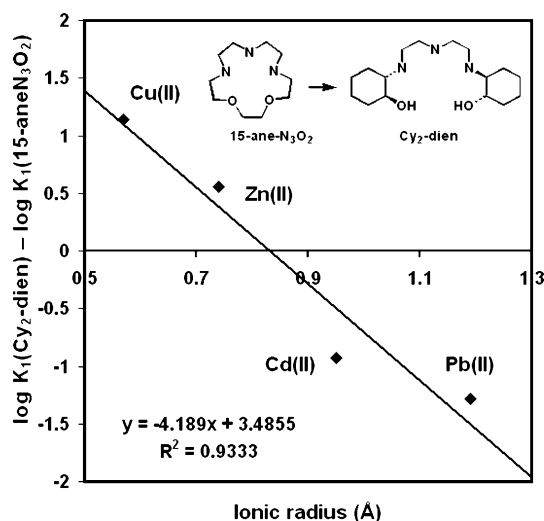
|                        | trans | cis   | trans | cis   |
|------------------------|-------|-------|-------|-------|
| <i>U</i> (free ligand) | 14.44 | 19.31 | 20.89 | 27.63 |
| <i>U</i> (ZnL)         | 24.50 | 26.54 | 34.99 | 43.21 |
| $\Delta U$ (Zn(II))    | 10.06 | 7.23  | 14.10 | 15.55 |
| $\Delta U$ (cis-trans) |       | -2.83 |       | +1.45 |
| <i>U</i> (CdL)         | 19.10 | 20.24 | 19.30 | 27.13 |
| $\Delta U$ (Cd(II))    | 4.66  | 0.93  | -1.59 | -0.05 |
| $\Delta U$ (cis-trans) |       | -3.73 |       | +1.44 |
| <i>U</i> (KL)          | 15.27 | 16.23 | 23.15 | 30.26 |
| $\Delta U$ (K(I))      | +0.83 | -3.08 | +2.26 | +2.63 |
| $\Delta U$ (cis-trans) |       | -4.91 |       | +0.37 |

<sup>a</sup> $\Delta U(M)$  refers to  $U_{ML}(U \text{ for the complex}) - U_L(U \text{ for the free ligand})$ , where M is Zn(II), Cd(II), or K(I). Units are kcal·mol<sup>-1</sup>.  $\Delta U(\text{cis-trans})$  shows for each pair of isomeric ligand complexes how much the cis isomer is sterically favored over the trans isomer.

is of some interest that the crossover of the *x* axis in Figure 8 occurs close to this value.

Log *K*<sub>1</sub> values for Cy<sub>2</sub>-tn were obtained only for Cu(II), Zn(II), and Cd(II) (Table 4), since the equilibria with Ni(II) were very slow and hindered measurement of log *K*<sub>1</sub>, whereas the Pb(II) complex did not form before the pH was so high that Pb(OH)<sub>2</sub> precipitated. The slow kinetics of the complex formation of Ni(II) with Cy<sub>2</sub>-tn is indicative of the high level of preorganization of the ligand, whereas the instability of the Pb(II) complex testifies to the ability of the six-membered chelate ring formed to lower the affinity of the ligand for large metal ions. The log *K*<sub>1</sub> values for Cy<sub>2</sub>-tn with Cu(II), Zn(II), and Cd(II) compared to Cy<sub>2</sub>-en show the exact pattern expected. Thus, log *K*<sub>1</sub> for the small Cu(II) ion increases on replacing the five-membered chelate ring between the two N donors of the Cy<sub>2</sub>-en complex with a six-membered chelate ring in the Cy<sub>2</sub>-tn complex. For the large Cd(II) ion, this causes a decrease in log *K*<sub>1</sub> in the Cy<sub>2</sub>-tn complex, as seen in Table 5. The log *K* values for the ligands studied here, namely, Cy<sub>2</sub>-dien, Cy<sub>2</sub>-en, and Cy<sub>2</sub>-tn, all refer to ligands where the cyclohexylene groups bridge between an N donor and an O donor. The effect on complex stability appears to be rather similar to that of ligands such as *trans*-CDTA, where the cyclohexylene group bridges between two N donors. The ligands studied by Hay et al.<sup>25</sup> involve chelate rings that contain neutral O donors. MM calculations are now discussed that address the questions raised in the introduction.

**MM Calculations.** The first question raised in the introduction, namely, why all neutral O-donor chelate rings

**Figure 7.** Effect of cyclohexylene bridges on metal-ion selectivity of N<sub>2</sub>O<sub>2</sub> donor set ligands, in plotting the difference in log *K*<sub>1</sub> between the Cy<sub>2</sub>-en (cyclohexylene bridges between N and O donors) and DHEEN (ethylene bridges between N and O donors) against metal ionic radii.<sup>15</sup> It is seen that the cyclohexylene bridges produce a larger increase in log *K*<sub>1</sub> for small metal ions (Cu(II)) than for large metal ions (Pb(II)). Ionic radii refer to octahedral radii except for Cu(II), for which the square-planar radius is given.**Figure 8.** Comparison of selectivity change ( $\Delta \log K$ ) of Cy<sub>2</sub>-dien compared with that of 15-aneN<sub>3</sub>O<sub>2</sub> as a function of metal-ion radius.  $\Delta \log K$  is log *K*<sub>1</sub> for the Cy<sub>2</sub>-dien complex minus log *K*<sub>1</sub> for the 15-aneN<sub>3</sub>O<sub>2</sub> complex. The diagram shows that the nonmacrocyclic Cy<sub>2</sub>-dien with its two cyclohexylene bridging groups between the donor atoms has more selectivity for smaller metal ions than does the macrocycle 15-aneN<sub>3</sub>O<sub>2</sub>. Ionic radii from ref 15 refer to octahedral radii except for Cu(II), for which the square-planar radius is given.

produce more stable complexes with cis substitution of the cyclohexenyl bridge and ligands with N donors form more stable complexes with trans substitution, can be addressed by MM calculations on model chelate rings with K(I), Cd(II), or Zn(II) as the metal ions. These were selected as examples of a very large, an intermediate, and a small metal ion. It should be noted that the same trend is observed with *cis*-*C,C'*-dimethyl (preferred with O donors) and *trans*-*C,C'*-dimethyl (preferred with N donors) substitution of the ethylene bridge of the chelate ring,<sup>19,26</sup> namely, that with two O donors, cis substitution leads to more stable complexes, whereas with two N donors, trans substitution does as well.

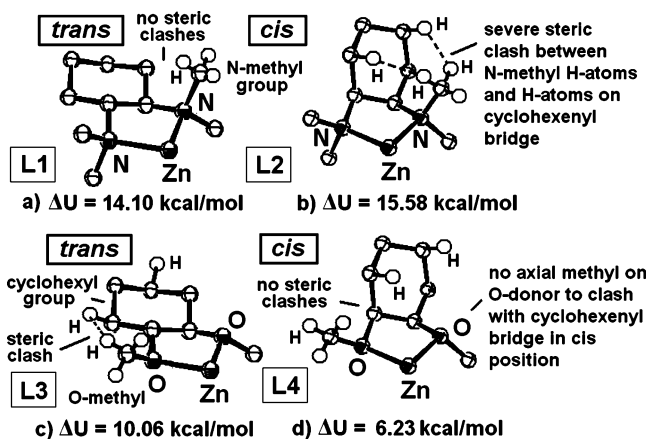


**Figure 9.** Structures of chelate rings of Zn(II), with cyclohexylene bridges between the donor atoms. See Figure 1 for structures of ligands L1–L4. (a) L1 has trans placement, and (b) L2 has cis placement of the  $-\text{NMe}_2$  donors on the cyclohexenyl bridge. (c) L3 has trans placement, and (d) L4 has cis placement (L4) of the O donors, whereas in parts a and b,  $\Delta U$  is lower for trans placement of the N donors (L1). Drawings were made with ORTEP;<sup>35</sup> short H–H nonbonded contacts ( $<2.4 \text{ \AA}$ ) are indicated with broken lines.

Calculations were carried out on model chelate rings, using the approach of Hay et al.,<sup>25</sup> with ligands L1–L4 in Figure 1. The results for the free ligands and the complexes with K(I), Cd(II), and Zn(II) are seen in Table 6. Ball-and-stick drawings of the chelate rings, together with the calculated increase in the strain energies on complex formation ( $\Delta U$ ), are seen in Figure 9. What the MM calculations allow one to identify is the source of the preference of chelate rings with neutral O donors for cis-substituted bridges and chelate rings with N donors for trans-substituted bridges. *It originates from the fact that the neutral O donor has only one substituent on it ( $-\text{OH}$  or  $-\text{OR}$ ), whereas the neutral N donor has two substituents on it ( $-\text{NH}_2$  or  $-\text{NR}_2$ ). For the N-donor ligands, one of the substituents has to occupy a sterically very unfavorable position in the cis-substituted ligand.* Thus, as seen in part b of Figure 9, the main problem that chelate rings involving a cyclohexenyl bridge with two *cis*- $\text{NMe}_2$  donor groups on it (L2 in Figure 1) have is a steric clash between the H atoms on the axial methyl of the  $-\text{NMe}_2$  group and the axial H atoms on the cyclohexenyl bridge. The O donor in part d of Figure 9 (L4 in Figure 1) has no such axial substituent and can accommodate the *cis*-cyclohexenyl bridge in a sterically efficient manner. In addition, it also does not have the steric clash between the  $-\text{OCH}_3$  group and the cyclohexenyl bridge that is present in L3 with its *trans*-substituted methoxy groups on the cyclohexenyl bridge, indicated in part c of Figure 9. The MM calculations summarized in Figure 9 thus account for  $\Delta U$  being less for the *cis*-substituted cyclohexenyl bridge with methoxy donor groups but also being less for the *trans*-substituted bridge with dimethylamino donor groups. This is in accordance with the preferences indicated by the formation constants.<sup>19,25,26</sup>

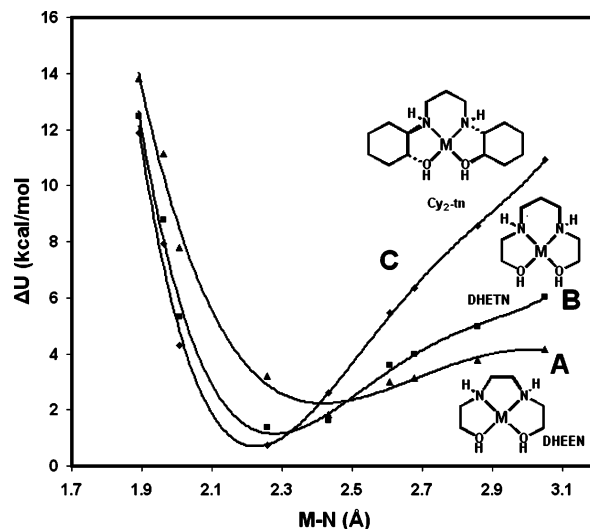


**Figure 10.** Increase in strain energy ( $\Delta U$ ) for the complexes of DHEEN (A) (five-membered chelate rings), DHETN (B) (one six-membered chelate ring), and its analogue  $\text{Cy}_2\text{-tn}$  (C) calculated as a function of M–N bond length using the MM+ module of *HyperChem* as described in the text.  $\Delta U = U(\text{ML})$  (the strain energy for the complex)  $- U(\text{L})$  (the strain energy of the free ligand). Note how the strain energy increases more rapidly with increasing metal-ion size for the cyclohexylene-bridged ligand at C than for the ethylene-bridged analogue at B, whereas  $U$  increases most slowly for A.

**Table 7.** Log  $K_1$  Values for en (Ethylenediamine) Complexes and with Ligands with Cyclohexylene-Substituted Bridges<sup>a</sup>

|                                | Co(II) | Ni(II) | Cu(II) | Zn(II) | Cd(II) |
|--------------------------------|--------|--------|--------|--------|--------|
| log $K_1$ (en)                 | 5.5    | 7.3    | 10.49  | 5.69   | 5.4    |
| log $K_1$ ( <i>cis</i> -DAC)   | 5.79   | 7.12   | 10.61  | 6.08   | 5.78   |
| log $K_1$ ( <i>trans</i> -DAC) | 6.37   | 7.80   | 11.09  | 6.37   | 5.80   |

<sup>a</sup> DAC = 1,2-diaminocyclohexane; data from ref 19.

In the situation where the substituents on the O donor or the N donor are H atoms rather than methyl groups, the steric interactions are much weaker. Thus, MM calculations show that the differences in  $\Delta U$  between *cis* and *trans* placements of the donor atoms on the cyclohexylene bridge shown in Figure 9 become much smaller, namely,  $\leq 1 \text{ kcal/mol}$ . This is in accordance (Table 7) with experimental values,<sup>19</sup> which show that the differences in log  $K_1$  are quite small for *cis*-1,2-diaminocyclohexane (*cis*-DAC) and *trans*-1,2-diaminocyclohexane (*trans*-DAC), where the substituents on the N donors are H atoms.

Point 2 raised above is the source of the shift in selectivity in favor of smaller metal ions induced by alkyl substituents on the ethylene bridges of chelate rings (see Figures 4, 7, and 8). This can be addressed by calculating  $\Delta U$  for DHETN and  $\text{Cy}_2\text{-tn}$  complexes as a function of metal-ion size, as shown in Figure 10. A curve for the DHEEN complex is also included as an example of an all five-membered set of chelate rings. Figure 10 shows that there is an increase in strain energy with an increase in metal-ion size for all three complexes, that is least for the DHEEN complexes with their five-membered chelate rings and increases for the DHETN and then the  $\text{Cy}_2\text{-tn}$  complexes, which have the largest increase in  $\Delta U$ . The large increase in the  $\text{Cy}_2\text{-tn}$  complexes can be traced to the short H–H nonbonded contacts, as seen in Figure 5 for the  $\text{Cy}_2\text{-tn}$  complex of Cu(II). These short



H–H contacts are predicted by MM to decrease from 2.28 Å in the complex with  $M-N = 1.9$  Å to 2.10 Å where  $M-N = 2.7$  Å. A reviewer has correctly pointed out that it appears that the parametrization of the H–H nonbonded repulsions in MM2 leads to H atoms where the repulsions are overestimated. Thus, the calculations reported here may be somewhat overestimated in Figure 10, for example. This has been corrected in the MM3 force-field,<sup>39</sup> but in general, the MM2 force field performs well, and it is not clear that overall better results are obtained by MM3 or even quantum-mechanical approaches. One should simply bear in mind that Figure 10 might somewhat overestimate the effects of short H–H nonbonded interactions at larger metal ionic radii.

The third question to be addressed, namely, why the chelating ligands containing N donors studied by us and others show increases in  $\log K_1$  on the addition of C-alkyl groups to the ethylene bridge whereas the crown ethers examined by Hay et al.<sup>25</sup> do not, can possibly be addressed in terms of preorganization<sup>40</sup> and inductive effects.<sup>41</sup> It appears<sup>41</sup> that the stabilization of the complexes of ligands by the placement of alkyl groups on ethylene bridges arises at least partly from a reduction in energy required to change the ethylene bridge from the anti conformation energetically favored in the free ligand to the syn conformation required to complex the metal ion. Since crown ethers are already more preorganized, with some or all of their ethylene bridges constrained in the syn conformation, this effect would not apply to them, and no stabilization would result, as is observed.<sup>25</sup> It is also possible that the N-donor ligands studied may respond better to the inductive effects of C-alkyl groups than do the O donors. A considerable amount of work has shown<sup>1,42</sup> that whether alkyl substituents will cause an increase in  $\log K_1$  or not is a balance between inductive and steric factors. Thus, for the types of metal ion studied with O donors, such as  $K^+$ , the response to the inductive effects of the substituents on the ethylene bridges of crown ethers is probably quite small, and so the adverse steric effects of the substituents (cyclohexylene and C-methyl groups) overcome the small inductive effects. In contrast, the types of metal ions studied with N-donor ligands, such as those reported here, are much more covalently bound and so will respond to the inductive effects of C-alkyl substituents on the bridges of ligands. Thus, for a C-alkyl substituent (R) on the ethylene bridge between the two N donors on EDTA, the reported<sup>19</sup>  $\log K_1$  values for Cu(II) are 18.78 (R = H), 19.82 (R = methyl), 20.6 (R = ethyl), and 21.1 (R = isopropyl), following the increased inductive-effect order of these substituents.<sup>1,42</sup> It should be noted, however, that this order is also the order of increasing bulk of the substituents;

hence, their increasing ability to favor the syn relative to the anti conformer leads to greater preorganization of the ligand for complexing metal ions.

## Conclusions

(1) The work reported here highlights the importance of short H–H nonbonded contacts in controlling metal-ion size-based selectivity. These are particularly important between C-alkyl substituents on the ethylene bridges of ligands and H atoms on substituents on the donor atoms, e.g., the methyl groups on ligands such as *trans*-1,2-dimethoxycyclohexane (L3 in Figures 1 and 9) or on bridging groups of additional chelate rings as in  $Cy_2$ -tn or CDTA complexes. It should be noted that when the donor atoms bear only H atoms as in –OH or –NH<sub>2</sub> groups, the steric effects are small. (2) In ligands with neutral O donors, *cis*-cyclohexylene bridges produce more stable complexes than *trans*-cyclohexylene bridges, whereas for N donors, the opposite is true. Where the N donors have two alkyl substituents (–NR<sub>2</sub>), one of these has to occupy an axial position on the chelate ring, where it clashes sterically with a *cis*-, but not a *trans*-cyclohexylene bridge. In contrast, neutral O donors can have only one substituent (–OR), and so there is no axial group to clash with the *cis*-cyclohexylene bridge, which is positioned in a sterically very efficient manner and produces more stable complexes than a *trans*-cyclohexylene bridge. The same analysis applies to the effects of C-methyl groups on the ethylene bridges of ligands in that, for two O donors, *cis* placement of 1,2-dimethyl groups will be preferred, whereas for N donors, *trans* placement of 1,2-dimethyl groups is preferred. (3) It appears that increasing inductive effects may contribute to increases in complex stability as more C-alkyl bridges are added to ethylene bridges. These inductive effects are strong for metal ions studied in the complexation of N-donor ligands, such as Cu(II), but are weak for metal ions such as K(I) studied in complexes with O-donor ligands. For the N-donor ligands, the inductive effects may outweigh the adverse steric effects produced by the C-alkyl substituents and  $\log K_1$  increases with increasing C-alkyl substituents, whereas for O-donor ligands and the very ionically bound metal ions such as K(I), adverse steric effects may predominate and  $\log K_1$  tends to decrease with increasing C-alkyl substituents on the bridging groups of the ligand. (4) The short H–H nonbonded contacts between the C-alkyl substituents on the bridge of the ligand and on adjacent substituents on the donor atoms (either C-alkyl groups or other chelate rings) become more severe as the size of the metal increases, and the curvature of the coordinated ligand decreases. This accounts for the increase in selectivity for smaller metal ions relative to that of larger metal ions, which results from placing C-alkyl substituents on the bridging groups of ligands.

**Acknowledgment.** We thank the University of North Carolina, Wilmington, the University of the Witwatersrand, and the H. E. Griffin Trust for the generous support of this work.

IC070239H

- (39) Lii, J.-H.; Allinger, N. L. *J. Am. Chem. Soc.* **1989**, *111*, 8576.  
 (40) Cram, D. J.; Kaneda, T.; Helgeson, R. C.; Brown, S. B.; Knobler, C. B.; Maverick, E.; Trueblood, K. N. *J. Am. Chem. Soc.* **1985**, *107*, 3645.  
 (41) Hancock, R. D.; Melton, D. L.; Harrington, J. M.; Dean, N. E.; McDonald, F. C.; Gephart, R. T.; Boone, L. L.; Jones, S. B.; Whitehead, J. R.; Cockrell, G. M. *Coord. Chem. Rev.*, in press.  
 (42) Hancock, R. D.; Nakani, B. S.; Marsicano, F. *Inorg. Chem.* **1983**, *22*, 2531.